RESEARCH

ARHGDIB as a prognostic biomarker and modulator of the immunosuppressive microenvironment in glioma

Xuejun Yan[1] · Rongnian Li[2] · Jing Xu[1] · Hua Liu[1] · Minmin He[1] · Xingjun Jiang[3] · Caiping Ren[4] · Quanwei Zhou[5]

Abstract

Background Glioma, a prevalent malignant intracranial tumor, exhibits limited therapeutic efficacy due to its immunosuppressive microenvironment, leading to a poor prognosis for patients. ARHGDIB is implicated in the remodeling of the tumor microenvironment and plays a significant role in the pathogenesis of various tumors. However, its regulatory effect within the immune microenvironment of glioma remains unclear.

Methods The mRNA expression pattern of ARHGDIB was analyzed using public databases, and its expression was further validated in our collected cohort through quantitative PCR (qPCR) and immunohistochemistry (IHC). Kaplan–Meier survival analysis and LASSO-Cox regression were employed to ascertain the clinical significance of ARHGDIB in glioma. Subsequently, we systematically evaluated the association between ARHGDIB expression and immune characteristics within the glioma microenvironment, as well as its potential to predict treatment response in glioma. Additionally, in vitro experiments were conducted to elucidate the role of ARHGDIB in remodeling the glioma microenvironment and promoting tumor malignancy progression.

Results Combined with bioinformatics analysis of public databases and validation with qPCR and IHC on our cohort, our findings indicate that ARHGDIB is markedly overexpressed in glioma and correlates with poor patient prognosis, thereby serving as a potential biomarker for adverse outcomes in glioma. Functional enrichment and immune infiltration analyses reveal that ARHGDIB is implicated in the recruitment of immunosuppressive cells, such as M2 macrophages and neutrophils, contributing to the alteration of the glioma immunosuppressive microenvironment and hindering the immune response. Further investigations through single-cell sequencing, immunohistochemistry, immunofluorescence, and in vitro experiments demonstrate that ARHGDIB exhibits an expression pattern akin to CD163, with its overexpression inducing M2 macrophage polarization and facilitating glioma cell proliferation and migration.

Conclusions ARHGDIB emerges as a novel marker for tumor-associated macrophages, playing a crucial role in shaping the immunosuppressive microenvironment and representing a promising prognostic biomarker for glioma.

Keywords Glioma · ARHGDIB · Immunosuppressive microenvironment · Tumor-associated macrophages · Prognosis

Xuejun Yan and Rongnian Li have been contributed equally to this work.

✉ Xuejun Yan
421698293@qq.com

✉ Xingjun Jiang
jiangxj@csu.edu.cn

✉ Caiping Ren
rencaiping@csu.edu.cn

✉ Quanwei Zhou
1091040044@qq.com

1 NHC Key Laboratory of Birth Defect for Research and Prevention, Hunan Provincial Maternal and Child Health Care Hospital, Changsha, Hunan, China

2 Xiangtan Hospital of Traditional Chinese Medicine, Xiangtan, Hunan, China

3 Department of Neurosurgery, Xiangya Hospital, Central South University, Changsha, Hunan, China

4 The NHC Key Laboratory of Carcinogenesis and The Key Laboratory of Carcinogenesis and Cancer Invasion of the Chinese Ministry of Education, School of Basic Medical Science, Central South University, Changsha, China

5 Department of Neurosurgery, The National Key Clinical Specialty, Zhujiang Hospital, Southern Medical University, Guangzhou, China

Introduction

Glioma represents a highly heterogeneous neoplasm within the central nervous system, exhibiting a relatively elevated incidence rate of approximately 6.4 cases per 100,000 individuals annually [1, 2]. Among these, glioblastoma multiforme (GBM) emerges as the most prevalent malignant subtype, constituting nearly 50% of all primary malignant central nervous system tumors [3]. Current therapeutic interventions for glioma primarily encompass surgical resection, chemotherapy, and radiotherapy. Despite the implementation of standard treatment protocols, such as surgical excision in conjunction with temozolomide chemotherapy or radiotherapy, the majority of glioma patients experience recurrence, particularly those diagnosed with GBM, recognized as the most malignant primary brain tumor [4]. Consequently, the overall prognosis for these patients remains poor. Prognostic outcomes for glioma patients exhibit significant variability depending on tumor grade, with median survival ranging from approximately 1 to 15 years [5]. Notably, only 3–5% of GBM patients survive beyond three years despite undergoing comprehensive treatment regimens, including surgical resection, chemotherapy, and radiotherapy, with most surviving approximately 14 months [6]. The immune microenvironment of gliomas and intratumoral heterogeneity are key factors leading to drug resistance, recurrence, and progression [7, 8]. For instance, tumor cells recruit macrophages into the central nervous system by secreting specific chemokines (such as MCP-1, CSF-1, and GM-CSF) and polarize them into a tumor-promoting phenotype [9–11]. The presence of this immunosuppressive microenvironment limits the efficacy of traditional immunotherapeutic strategies (such as PD-1/PD-L1 inhibitors) in the treatment of gliomas. Targeting key molecules or cells within the tumor microenvironment, in combination with surgery, radiotherapy, and chemotherapy, holds promise for improving the clinical outcomes of glioma treatment, prolonging patient survival, and enhancing quality of life.

ARHGDIB (also known as RhoGDI2), a member of the Rho GDP dissociation inhibitor family, is a regulatory protein that primarily controls the activity of small GTPases in the Rho family by binding to them. Rho family GTPases play a crucial role in cellular morphological changes, migration, proliferation, and cytoskeletal reorganization [12–14]. Recent studies have found that ARHGDIB indirectly affects tumor invasion and metastasis by regulating multiple signaling pathways, exerting a dual role in different tumors by either promoting or inhibiting tumor invasion and metastasis. For example, in lung cancer, bladder cancer, and Hodgkin's lymphoma, overexpression of ARHGDIB can inhibit the metastasis and invasion of tumor cells [15–17], whereas in gastric cancer, breast cancer, and colorectal cancer, overexpression of ARHGDIB promotes the metastasis and invasion of tumor cells [18–20]. Studies have reported that ARHGDIB inhibits the metastasis of bladder cancer by suppressing the Rac1 pathway and affects the invasion [17] and proliferation of lung cancer and hepatocellular carcinoma cells by modulating the PI3K/Akt signaling pathway [15, 21]. In ovarian cancer, ARHGDIB enhances Rac1 activity to activate the p38 and JNK/MAPK cascades, thereby inhibiting tumor metastasis [22]. In breast cancer, high expression of ARHGDIB is positively correlated with the poor prognosis of the patient, lymph node metastasis, and TNM staging and promoted tumor invasion by regulating epithelial–mesenchymal transition (EMT) and the expression of MMP2 [23]. In addition, ARHGDIB promotes chemoresistance in gastric cancer cells through multiple mechanisms, including upregulation of Bcl-2 and activation of PLCγ [24, 25]. Moreover, the role of ARHGDIB in the tumor immune microenvironment is gradually gaining attention. It has been reported that ARHGDIB suppresses lung metastasis in mice with muscle-invasive bladder cancer by reducing tumor versican expression and macrophage infiltration [26], indicating that ARHGDIB is also involved in remodeling the tumor microenvironment. The aforementioned studies highlight the role of ARHGDIB in tumor progression, involving tumor proliferation, invasion, metastasis, and remodeling of the tumor microenvironment, suggesting that ARHGDIB is a potential therapeutic target for cancer. However, few studies have reported on the role of ARHGDIB in gliomas, such as its expression levels, prognostic value, and impact on the immune microenvironment of gliomas. Therefore, it is necessary to reveal the relationship between ARHGDIB and glioma progression and elucidate its potential as a therapeutic target, providing new insights for improving the clinical therapeutic outcomes of gliomas.

In this study, we employed high-throughput sequencing technology, bioinformatics analysis, and in vitro experiments to discover that ARHGDIB is highly expressed in gliomas and is closely related to the malignant phenotype of gliomas, serving as a biomarker for poor prognosis in gliomas. ARHGDIB exhibits a similar expression pattern to CD163 and is involved in remodeling the immune microenvironment of gliomas. The aberrantly expressed ARHGDIB recruits the infiltration of M2 macrophages, forming an immunosuppressive microenvironment that promotes the malignant progression of the tumor. Additionally, the expression of ARHGDIB is correlated with immune checkpoint molecules such as PD-1/PD-L1 and the immunotherapy pathway. These findings provide important evidence for a deeper understanding of the mechanisms by which ARHGDIB contributes to glioma

progression and offers new targets and strategies for the treatment of gliomas.

Materials and methods

Obtaining and processing data

The approaches employed for data acquisition and processing align with those detailed in prior studies [27, 28]. All data were retrieved from Chinese Glioma Genome Atlas (CGGA) datasets (CGGA-693, CGGA-325, CGGA-301), TCGA, GSE16011, and Rembrandt datasets.

Clinical specimens

For the in-house cohorts, we included 200 patients who were newly diagnosed with glioma and underwent craniotomy at Xiangya Hospital, Central South University, from 2015 to 2022. All patients had at least one month of follow-up. After excluding those with incomplete data, a total of 200 patients were included in the subsequent analysis. Written informed consent was obtained from each participant, and the study was approved by the ethics committee.

RNA extraction and quantitative real-time PCR

We conducted these procedures by referring to the previous study [29]. In brief, total RNA was extracted from fresh tissue using TRizol reagent (Life Technologies) following the manufacturer's protocol. Complementary DNA was synthesized from the extracted RNA using a reverse transcription kit (Thermo Fisher Scientific). Real-time quantitative PCR (qPCR) was performed using SYBR qPCR Master Mix (Vazyme). ACTB was used as the internal reference gene, and the relative expression levels of ARHGDIB, CD163, ARG1, and TGF-β1 were quantified using the $2^{-\Delta\Delta Ct}$ method. The primer sequences are listed below:

ARHGDIB forward primer: GAGGCACGTACCACA ACAAGTC,

ARHGDIB reverse primer: TCATTCTGTCCACTCCTT CTTAATCG,

CD163 forward primer: AAAGAATCCCGCATTTGG CAGTG,

CD163 reverse primer: ATAACTCCCGCATCCTCC TTGTG,

ARG1 forward primer: GGCAGAAGTCAAGAAGAA CGGAAG,

ARG1 reverse primer: CTTGTGGTTGTCAGTGGAGTG TTG,

TGF-β1 forward primer: GCAACAATTCCTGGCGAT ACCTC.

TGF-β1 reverse primer: CCTCCACGGCTCAACCAC TG.

ACTB forward primer: GGCCAACCGCGAGAAGAT GAC,

ACTB reverse primer: GGATAGCACAGCCTGGAT AGCAAC.

Immunohistochemistry and immunofluorescence

A tissue microarray (TMA) was constructed using 17 normal tissue samples and 165 glioma tissue samples. Following the methodology described in the previous literature [30], we conducted the experiments. IHC and IF assays were performed using primary antibodies against ARHGDIB (Abcam, AB181252-1003) and CD163 (Abcam, AB182422-1003).

Survival analysis

Initially, we excluded samples with overall survival (OS) of less than 30 days and those lacking complete clinical characteristic data. Kaplan–Meier method was employed to estimate the association between ARHGDIB mRNA expression levels and patient outcomes, including OS, disease-specific survival (DSS), and progression-free interval (PFI); a *p* value of less than 0.05 was considered statistically significant.

Identification and functional enrichment analysis of differentially expressed genes

Patients were categorized into high and low ARHGDIB expression groups based on the median expression level of ARHGDIB. Using the limma package of R, differentially expressed genes (DEGs) related to ARHGDIB were identified between the two groups in the TCGA cohorts. The criteria for identifying DEGs were set as adjusted $P < 0.05$ and |log2(fold change)|> 1. Functional enrichment analysis was performed using the module of Gene set enrichment analysis (GSEA) on the Xiantao academic platform (https://www.xiantaozi.com) to elucidate the potential mechanisms underlying ARHGDIB.

Characteristics of the immune landscape in the glioma microenvironment

The immune and stromal scores were calculated using the ESTIMATE package of R [31]. The immunological landscape of the glioma microenvironment was comprehensively evaluated by examining the expression levels of immunomodulatory molecules, the infiltration levels of tumor-infiltrating immune cells (TIICs), the activity of the tumor immunity cycle, and the expression of inhibitory immune

checkpoints. Data for a total of 122 immunomodulators, including MHC molecules, chemokines, and immune stimulators, were sourced from prior studies [32]. The activity of the tumor immunity cycle was assessed through single-sample gene set enrichment analysis (ssGSEA) based on gene expression profiles [33]. The abundance of TIICs was estimated using ssGSEA and CIBERSORT algorithms [34]. Additionally, we identified 20 immunosuppressive checkpoints with potential therapeutic relevance, based on Auslander's study [35].

Development and validation of an ARHGDIB-associated risk score via LASSO regression

In TCGA, CGGA-325, CGGA-301, CGGA-693, and Rembrandt cohorts, univariate Cox regression analysis was conducted on the differentially expressed genes (DEGs) using the survival R package. A prognostic model associated with ARHGDIB was developed by employing the LASSO regression method to identify 13 prognostic markers from the 139 ARHGDIB-related DEGs that were significantly associated with prognosis. Individual risk scores were calculated using the Cox regression coefficients (β) and mRNA expression levels. The TCGA cohort was split into training and validation sets in a 7:3 ratio. An R package was utilized to evaluate the statistical performance of the prognostic model. Furthermore, the ARHGDIB-associated risk score was validated as a prognostic indicator in multiple datasets, including the TCGA internal validation set, TCGA-all set, CGGA-693 set, CGGA-301 set, CGGA-325 set, and Rembrandt dataset.

In vitro functional experiments

Cell culture was performed according to previously published protocols [28]. Briefly, THP-1 cells were cultured in RPMI-1640 medium supplemented with 10% fetal bovine serum (FBS), while T98G and U87 cells were maintained in DMEM medium containing 10% FBS. All cells were incubated at 37 °C in a humidified atmosphere with 5% CO_2.

Co-culture model: THP-1 cells were induced into M0-type macrophages using PMA (50 ng/mL) for 24 h [36]. Subsequently, these M0 macrophages were infected with lentiviruses carrying the ARHGDIB expression vector or control vector. After 48 h, the cell supernatant was collected and co-cultured with T98G and U251 cells. After two days of co-culture, the cells were harvested for subsequent experiments, including CCK-8, colony formation, and migration assays.

CCK-8, colony formation, and migration assays: These experiments were conducted following previously published literature [29]. In brief, after a 2-day co-culture of T98G and U251 cells with M0-oE-ARHGDIB or M0-oE-Vector, then

T98G and U251 cells were collected. For CCK-8, the cells were plated into 96-well plates at a density of 1000 cells/well in 100 μL of complete medium and cultured at 37 °C. Upon completion of each experiment, 10 μL of CCK-8 reagent (Beyotime, Shanghai, China) was added to each well, followed by an additional 2-h incubation at 37 °C; then, the optical density (OD450) was subsequently measured using a microplate reader. For colony formation, the cells were plated into 6-well plates at a density of 1000 cells/well; after culturing for 2 weeks, the cells were fixed with paraformaldehyde stained with 0.1% crystal violet and observed under a microscope. For migration assays, cells (20,000 cells/transwell) were added to the transwell upper chambers (8 μm) and cultured in a low-serum concentration (1.0%), after two days of incubation, the Transwell inserts were removed, and a cotton swab was used to gently wipe away the cells that had not migrated through the membrane, and then the cells were fixed with paraformaldehyde stained with 0.1% crystal violet and observed under a microscope.

Statistical analysis

All statistical analyses were performed using GraphPad Prism 8.0.2 or R software (www.r-project.org). The unpaired t test was employed to assess the expression of ARHGDIB between the normal and tumor groups, as well as between the IDH mutant and wild-type groups. The Kruskal–Wallis test was used to compare nonparametric differences among various histological subtypes. Pearson correlation analysis was conducted to evaluate the correlation between ARHGDIB expression levels and immune checkpoint molecules, immune scores, and stromal scores. A *p* value of less than 0.05 was considered statistically significant. The symbols *, **, and *** denote *p* values less than 0.05, 0.01, and 0.001, respectively.

Results

Identification and validation of a novel biomarker in glioma

To identify new biomarkers in gliomas, we collected six paired gliomas and adjacent tissues for RNA high-throughput sequencing. The result indicated that 2378 genes were significantly upregulated and 2336 genes were significantly downregulated (LogFC ≥ 1 or LogFC ≤ -1, *P* < 0.05, Fig. 1A). Similarly, the differential gene expression analysis of TCGA and GSE16011 cohorts, respectively, identified 6563 and 2612 genes (Log FC ≥ 1 or Log FC ≤ -1, *P* < 0.05, Fig. 1 B, C). Finally, combined with the above analysis results, 371 common upregulated genes were identified (Fig. 1D). After reviewing the literature, we finally
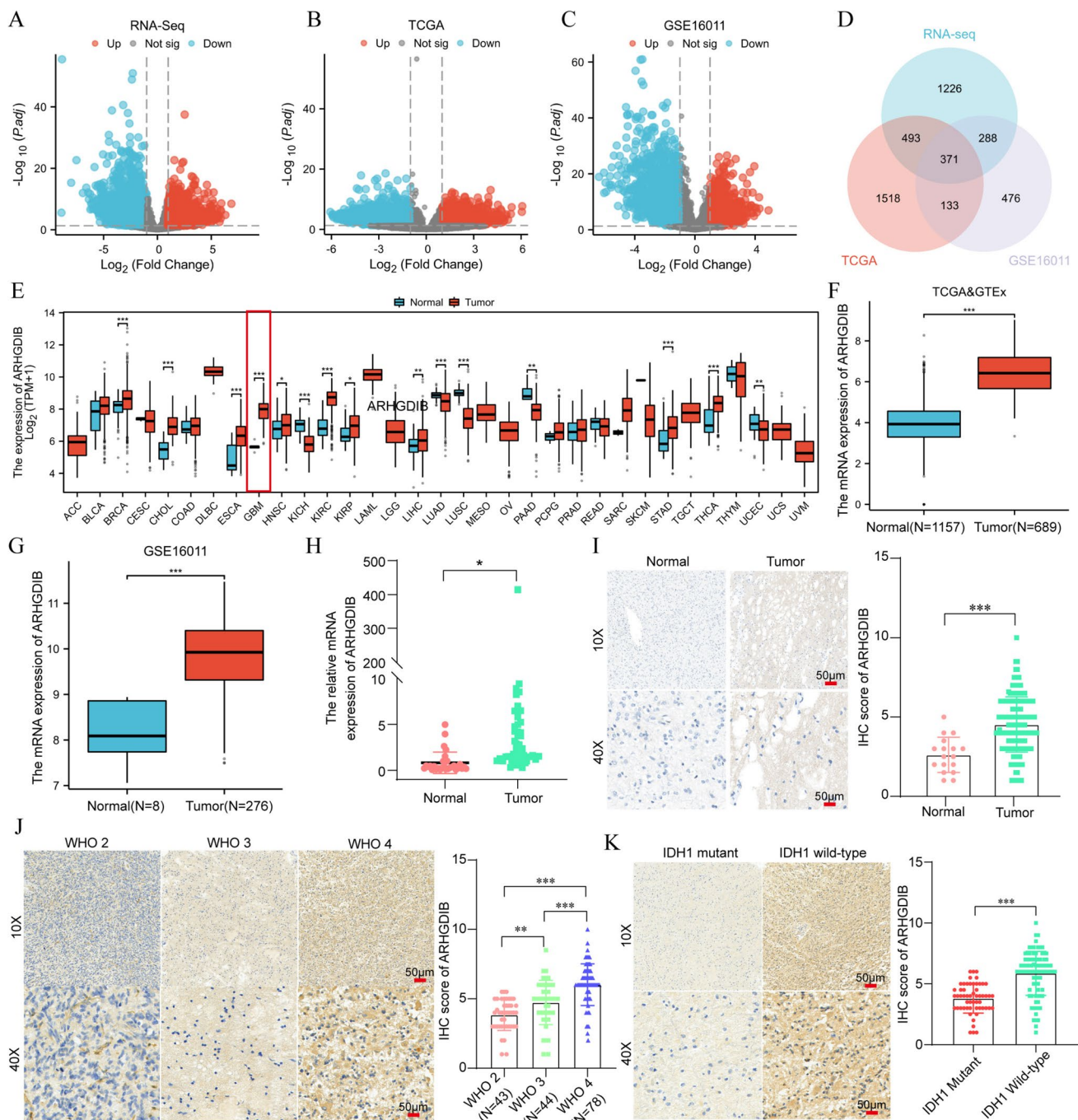
Fig. 1 ARHGDIB is abnormally highly expressed in gliomas. **A–C** The volcano plot shows differentially expressed genes (DEGs) in Our sequencing data, TCGA, and GSE16011 cohort. **D** The Venn diagram of upregulated genes intersects. **E** A pan-cancer analysis of ARHGDIB expression differences between normal samples and tumor tissues using the TCGA database. **F** and **G** The expression levels of ARHGDIB in normal tissues and glioma tissues were analyzed using the combining GTEx data with TCGA data, and the GSE16011 dataset. **H** The mRNA expression levels of ARHGDIB in normal tissues and glioma tissues were detected by qPCR in our own collected cohort. **I–K** The protein expression levels of ARHGDIB in normal tissues and glioma tissues (**I**), gliomas of different WHO grades (**J**), and tissues with wild-type and mutant IDH1 (**K**) were detected by immunohistochemical staining. Differences between the two groups were assessed using Student's t test, with P values indicated above each boxplot using asterisks (scale bar: 50 µm, *$P<0.05$, **$P<0.01$, ***$P<0.001$)

determined that ARHGDIB should be the object of further study. To assess the expression of ARHGDIB in tumors, we conducted a pan-cancer analysis of the expression of ARHGDIB and found that it is highly expressed in various tumor tissues, including glioblastoma multiforme (GBM), a highly malignant subtype of glioma (Fig. 1E). By combining GTEx data with TCGA data, we successfully increased the number of normal tissue samples. The levels of ARHGDIB in various tumor tissues, including low-grade glioma (LGG) and GBM tissues, were significantly higher than those in non-tumor tissues. (Fig. 1F). We analyzed the expression of ARHGDIB in other datasets, such as the GSE16011 cohort (Fig. 1G) and Rembrandt cohort (Figure S1A), and obtained consistent results. Then, we collected 64 glioma tissues and 30 normal tissue samples and examined the expression level of ARHGDIB by RT-qPCR. We also explored the expression level of ARHGDIB by IHC in two tissue microarrays (TMA) containing 165 diffuse gliomas and 17 normal samples. Those results consistently show ARHGDIB was highly expressed in the glioma tissues, compared with normal tissues (Fig. 1H, I, $P < 0.05$). To further investigate the expression patterns of ARHGDIB in glioma, we analyzed its expression in different WHO grades and IDH mutation statuses across various datasets. In the TCGA dataset, ARHGDIB was upregulated in glioma with WHO grade IV (Figure S1B, $P < 0.05$) and wild-type IDH

glioma (Figure S1C, $P < 0.05$), which was validated in the CGGA-693, GSE16011 and Rembrandt cohorts ($P < 0.05$, Figures S1D–H). The above results were validated by IHC in the validation dataset (Fig. 1J, K, $P < 0.05$). Furthermore, ARHGDIB was markedly over-expressed in 7 paired tumor tissues, in comparison with corresponding peritumoral tissues (Figure S2, $P < 0.05$). Consequently, these findings imply that ARHGDIB could function as a novel biomarker for the malignant characteristics of gliomas.

ARHGDIB is an indicator of poor prognosis in glioma

Survival curves were employed to investigate the prognostic significance of ARHGDIB expression in glioma across the six cohorts, and the findings consistently demonstrated that ARHGDIB serves as a marker of unfavorable prognosis in glioma (TCGA, HR = 3.57 (2.73–4.66); CGGA-693, HR = 2.33 (1.89–2.86); CGGA-301, HR = 1.79 (1.33–2.40); CGGA-325, HR = 2.72 (2.05–3.61); GSE16011, HR = 1.75 (1.34–2.27); Rembrandt, HR = 1.81 (1.44–2.29); log-rank test $P < 0.05$, Fig. 2A–F). When delving deeper into the correlation between ARHGDIB expression and disease-specific survival (DSS) as well as progression-free survival (PFS), patients exhibiting elevated levels of ARHGDIB were observed to experience reduced survival durations (DSS, HR = 3.87 (2.90–5.15); PFS, HR = 2.91 (2.33–3.65),
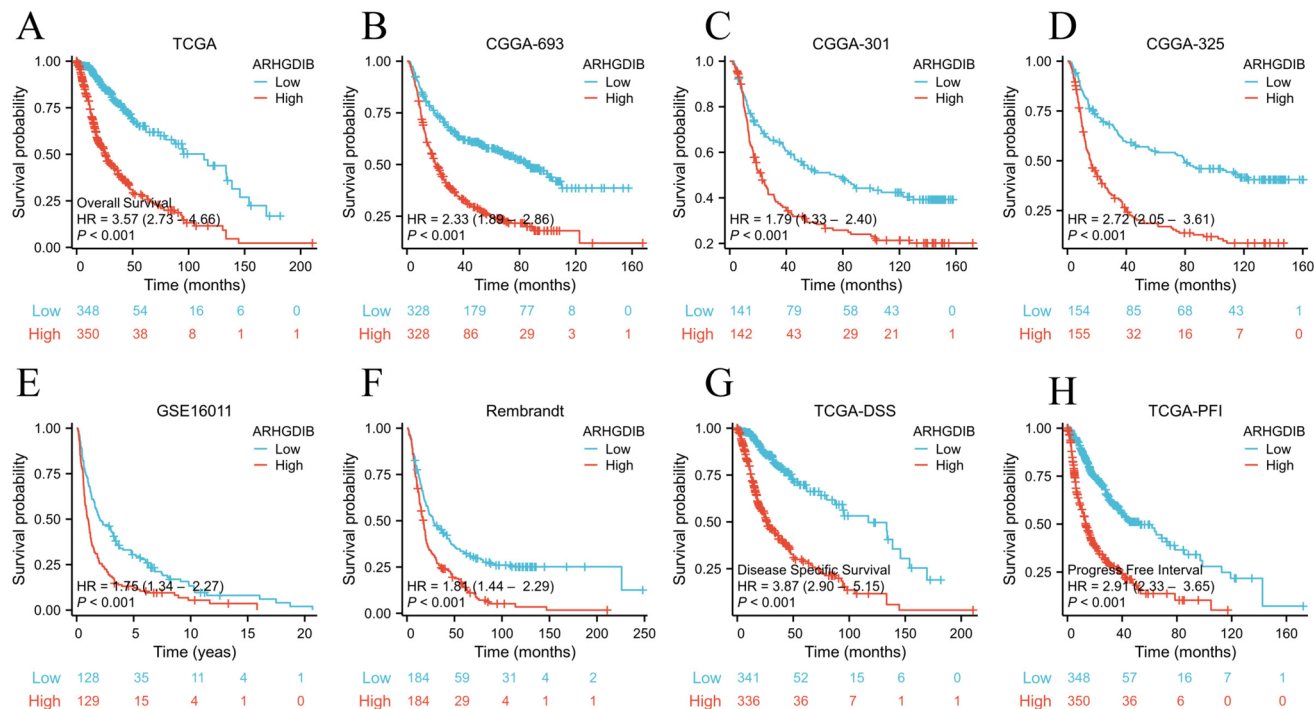

Fig. 2 ARHGDIB serves as an adverse prognostic biomarker in glioma. **A–F** Kaplan–Meier curves illustrating the associations between ARHGDIB expression and overall survival (OS) in glioma patients across multiple datasets: TCGA (**A**), CGGA-693 (**B**), CGGA-301 (**C**), CGGA-325 (**D**), GSE16011 (**E**), and Rembrandt (**F**). **G** and **H** Kaplan–Meier curves demonstrating the associations between ARHGDIB expression and disease-specific survival (DSS) and progression-free interval (PFI) in TCGA cohort

log-rank test $P < 0.05$, Fig. 2G, H). In addition, we investigated the relationship between the expression levels of ARHGDIB and patient survival outcomes, including overall survival, DSS, and PFS, in various subgroups of glioma, such as different grades of glioma and IDH status. The findings consistently indicated that elevated expression levels of ARHGDIB were linked to a worse prognosis in patients (Figure S3). Moreover, we explored the value of ARHGDIB in the diagnosis and prognostic evaluation of glioma patients based on TCGA, and the results showed that the AUC of the diagnostic ROC curves for distinguishing tumor from normal tissue and for tumor WHO grading was 0.879 (CI = 0.833–0.925) and 0.859 (CI = 0.829–0.890), respectively, and the AUC of the time-dependent ROC curves at 1, 3, and 5 years was 0.791, 0.753, and 0.706, respectively (Figure S4). In summary, the expression level of ARHGDIB can accurately distinguish normal tissue from glioma tissue and can also make a good prediction of patient prognosis. The higher the expression level of ARHGDIB, the worse the patient's prognosis, indicating that ARHGDIB is a potential adverse prognostic biomarker for glioma patients.

The correlations of ARHGDIB with immunological parameters

Given that the expression levels of ARHGDIB are intricately associated with the severity of glioma, we deduced that the abnormal expression of ARHGDIB might potentially facilitate the advancement of glioma. To explore the relationship between ARHGDIB and the progression of glioma, we first divided the glioma samples in the TCGA database into high and low-expression groups based on the expression level of ARHGDIB and conducted differential analysis. A total of 2138 genes were significantly upregulated, and 1135 genes were downregulated (Fig. 3A). Then, we performed GSEA enrichment analysis on the highly expressed genes to explore the potential signaling pathways affected by ARHGDIB. Gliomas that displayed elevated levels of ARHGDIB demonstrated significant enrichment in various immunomodulatory pathways, which included critical processes such as "angiogenesis," "inflammatory response," "TNFα-NF-kappaB signaling," and "IL2/STAT5 signaling," as observed in the comprehensive analysis of the TCGA cohort (Fig. 3B). Furthermore, the intricate and multifaceted microenvironment of glioma was meticulously assessed through the application of the ESTIMATE algorithm; we found that gliomas with high levels of ARHGDIB consistently exhibited higher immune and stromal scores than those with low levels of ARHGDIB in six cohorts ($P < 0.05$, Fig. 3C–H), indicating that ARHGDIB may play a regulatory role in the functioning of both immune and stromal cells. We also assessed cell infiltration in 33 cancers using CIBERSORT and ssGSEA algorithms; the results of CIBERSORT show that in GBM

and LGG, significant correlations can be observed between ARHGDIB and various types of immune cells, especially in GBM, the expression levels of ARHGDIB show significant positive correlations with M2 macrophages, regulatory Tregs, and other cells while showing negative correlations with activated NK cells and naive CD4 T cells, and the results of ssGSEA show that in GBM and LGG, the expression levels of ARHGDIB are significantly positively correlated with the infiltration levels of various immune cells, including aDCs (activated dendritic cells), B cells, CD8 T cells, neutrophils, mast cells, and macrophages ($P < 0.05$, Fig. 3I, J). These results indicated that ARHGDIB plays an important role in the immune microenvironment of gliomas. Importantly, ARHGDIB expression was positively correlated with infiltration of M2 macrophages in the TCGA, CGGA-301, and Rembrandt cohorts and negatively correlated with infiltration of Treg cells ($P < 0.05$, Fig. 3K–M). The ssGSEA analysis of the TCGA cohort shows that glioma tissues with high expression of ARHGDIB have a greater infiltration of immune-suppressive cells, such as macrophages and neutrophils, dendritic cells ($P < 0.05$, Fig. 3N). The same results were also observed in other cohorts, such as CGGA-693, CGGA325, CGGA-301, Rembrandt, and GSE16011 ($P < 0.05$, Fig. 3O–S). In summary, ARHGDIB plays a vital role in the tumor microenvironment, which forms an immunosuppressive tumor microenvironment, promoting the malignant progression of glioma.

The correlations of ARHGDIB with tumor immune response

Considering that ARHGDIB plays an important role in constructing the immunosuppressive microenvironment of glioma, we further analyze its relationship with tumor immune response. We first analyzed the distribution of 122 immune regulatory molecules, such as chemokines, receptors, MHC, and immunostimulators in the high and low-expression groups of ARHGDIB based on TCGA. In the high-ARHGDIB group, the majority of MHC molecules were markedly overexpressed, suggesting an improved capacity to present and process antigens. In addition, the concentrations of CXCL9, CXCL10, and CCR3, which enhance the recruitment of CD8 + T cells into the glioma microenvironment, were elevated in gliomas exhibiting high ARHGDIB expression. Chemokines and their corresponding receptors, including CCL2 and CCR2, were upregulated in gliomas expressing ARHGDIB (Fig. 4A). Furthermore, most immune cell markers were elevated in the high-ARHGDIB group in contrast to the low-ARHGDIB group (Fig. 4B). Then, we further explored the condition of the immune cycle. The cancer immunity cycle comprises seven stages: the release of cancer cell antigens (Step 1), cancer antigen presentation (Step 2), priming and activation (Step 3), the trafficking of immune
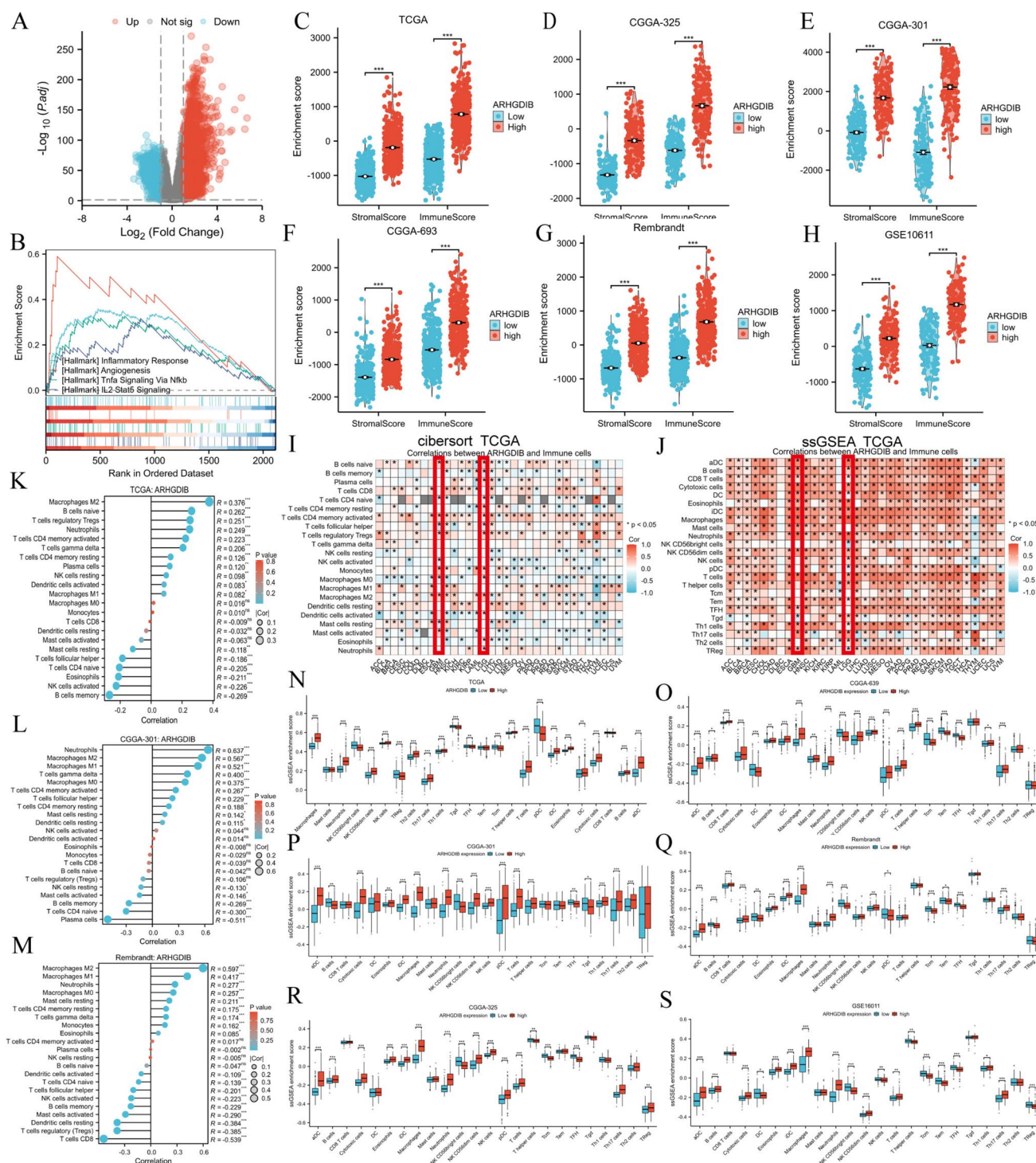
cells to tumors (Step 4), infiltration of immune cells into tumors (Step 5), recognition of cancer cells by T cells (Step 6), and the destruction of cancer cells (Step 7). The efficacy of the tumor immune cycle is a direct consequence of the operation of the chemokine system and immunomodulators. In the high-ARHGDIB group, the activities of the majority of steps were diminished, encompassing Step 1, Step 3, and Step 4 (macrophage recruitment, Th1 cell recruitment, NK cell recruitment, and Th17 recruitment) (Fig. 4C). Finally, we analyzed the correlation between ARHGDIB and immune checkpoint molecules, as well as its relationship with immunotherapy-related pathways. The expression level of ARHGDIB in gliomas is highly positively correlated with most immune checkpoint molecules, including LAIR1,

◀**Fig. 3** ARHGDIB reshapes the immunosuppressive microenvironment in glioma. **A** The volcano plot illustrates the DEGs between the low-ARHGDIB and high-ARHGDIB groups in TCGA glioma cohort. **B** GSEA analysis was performed on gliomas with low and high ARHGDIB expression in TCGA cohort; the significance of the enrichment score (ES) was determined using thresholds of a nominal $P < 0.05$ and an FDR < 25%. (C-H) The ESTIMATE algorithm evaluates the stromal and immune scores in high- vs. low-ARHGDIB groups across multiple cohorts: **C** TCGA, **D** CGGA-325, **E** CGGA-301, **F** CGGA-693, **G** Rembrandt, **H** GSE16011. **I** and **J** Pan-cancer analysis of the correlation between ARHGDIB expression levels and immune cell infiltration using the CIBERSORT and ssGSEA algorithms. **K** and **M** The lollipop plot illustrates the correlation between ARHGDIB expression levels and the abundance of immune cell infiltration in glioma, based on CIBERSORT algorithms from TCGA (**K**), CGGA-301 (**L**), Rembrandt cohort (**M**). **N–S** The ssGSEA algorithm was used to evaluate the levels of immune cell infiltration in gliomas of high- vs. low-ARHGDIB groups across multiple cohorts: **N** TCGA, **O** CGGA-693, **P** CGGA-301, **Q** CGGA-325, **R** Rembrandt, **S** GSEA10611. Differences between the two groups were assessed using Student's t test, with P values indicated above each boxplot using asterisks (**$P < 0.01$, ***$P < 0.001$)

PDCD1, CD274, CD44, and CTLA-4 (Fig. 4D). Moreover, the ARHGDIB expression exhibited a positive correlation with the ssGSEA scores of the majority of immunotherapy-related signatures (Fig. 4E). These research findings suggest that ARHGDIB shapes an inflamed tumor microenvironment, which inhibits the immune response in gliomas.

Development, verification, and assessment of the ARHGDIB-related risk score

In this investigation, we uncovered 678 overlapping ARHGDIB-related DEGs in the CGGA-693, CGGA-325, CGGA-301, Rembrandt, and TCGA cohorts. Among these DEGs, we also discerned 139 ARHGDIB-associated DEGs that were significantly correlated with prognosis (Table S1). Then, the LASSO Cox regression model was utilized to identify the 13 most significant factors for constructing a prognostic model in the TCGA training set and to derive an ARHGDIB-associated risk score for each patient based on the mRNA expression of thirteen genes and the corresponding LASSO Cox coefficients (Fig. 5A, B, Table S2). Patients with low-risk scores exhibited markedly prolonged overall survival durations compared to those with high-risk scores in the TCGA training set, TCGA internal validation set, and TCGA set (TCGA training set, HR = 7.51 (4.85–11.62), $P < 0.001$; TCGA validation set, HR = 5.17 (3.05–8.75), $P < 0.001$; TCGA set, HR = 6.05 (4.35–8.41), $P < 0.001$, Fig. 5C–E). The CGGA-693, CGGA-325, CGGA-301, and Rembrandt sets were employed as external validation sets. The findings demonstrated that the risk score could proficiently categorize patients into two separate groups within these external validation cohorts. Patients in the high-risk group exhibited a markedly worse prognosis compared to those in the low-risk group

(CGGA-693, HR = 3.23 (2.62–3.99), $P < 0.001$; CGGA-325, HR = 5.09 (3.76–6.88), $P < 0.001$; CGGA-301, HR = 2.82 (2.08–3.82), $P < 0.001$; Rembrandt, HR = 3.05 (2.40–3.87), $P < 0.001$, Fig. 5F–I). The predictive precision of the risk score was thoroughly corroborated in the TCGA training cohort, TCGA internal validation cohort, and TCGA dataset. The AUC of the risk score exceeded 0.80 for survival at 1, 3, and 5 years in the TCGA training cohort, TCGA internal validation cohort, and TCGA dataset (Fig. 5J–L). Similarly, the AUC of the risk score was more than 0.75 for survival at 1, 3, and 5 years in the CGGA-693 cohort, CGGA-325, CGGA-301, and Rembrandt cohort (Fig. 5H–O). These research results indicate that a model constructed based on ARHGDIB-related genes can effectively predict the prognosis of glioma patients.

Aberrant ARHGDIB expression was associated with M2 macrophages

Considering that the expression of ARHGDIB is highly correlated with immune cell infiltration in gliomas, we performed single-cell sequencing analysis based on GSE182109 and identified four cell types (Fig. 6A) and further analyzed the distribution of ARHGDIB and markers of M2 macrophages, such as CD163, VSIG4, CD14, SOX2, OLIG1, S100B, and glioma cells in cell clusters (Fig. 6B), the results uncovered that ARHGDIB and CD163, a marker of M2 macrophages, shared a similar expression pattern. To further substantiate these findings, we analyzed the correlation between ARHGDIB and CD163 expression based on the TCGA and CGGA-301 databases and conducted an immunohistochemistry experiment. The results showed a strong correlation between the expression of ARHGDIB and CD163, with correlation coefficients of 0.688 and 0.701 in TCGA and CGGA-301, respectively (Fig. 6C, $P < 0.001$), and in glioma tissue, gliomas with high-expression ARHGDIB exhibited high-expression CD163 by IHC (R = 0.474, $P < 0.001$, Fig. 6D). Moreover, the immunofluorescence experimental results based on glioma tissues showed co-localization between ARHGDIB and CD163 (Fig. 6E). These results suggested that the abnormal expression of ARHGDIB may promote the infiltration of more M2 macrophages into glioma tissues. To investigate the impact of ARHGDIB-mediated recruitment of M2 macrophage infiltration on the malignant progression of glioma, we conducted in vitro cell experiments. We induced THP-1 cells into M0 macrophages using PMA, transfected them with an ARHGDIB expression plasmid, and then co-cultured them with glioma cells to examine the proliferation and migration capabilities of the glioma cells. The results showed that the mRNA expression of TGFB1, CD163, and ARG1 in M0 macrophages overexpressing ARHGDIB was increased when these M0 macrophages cocultured with glioma
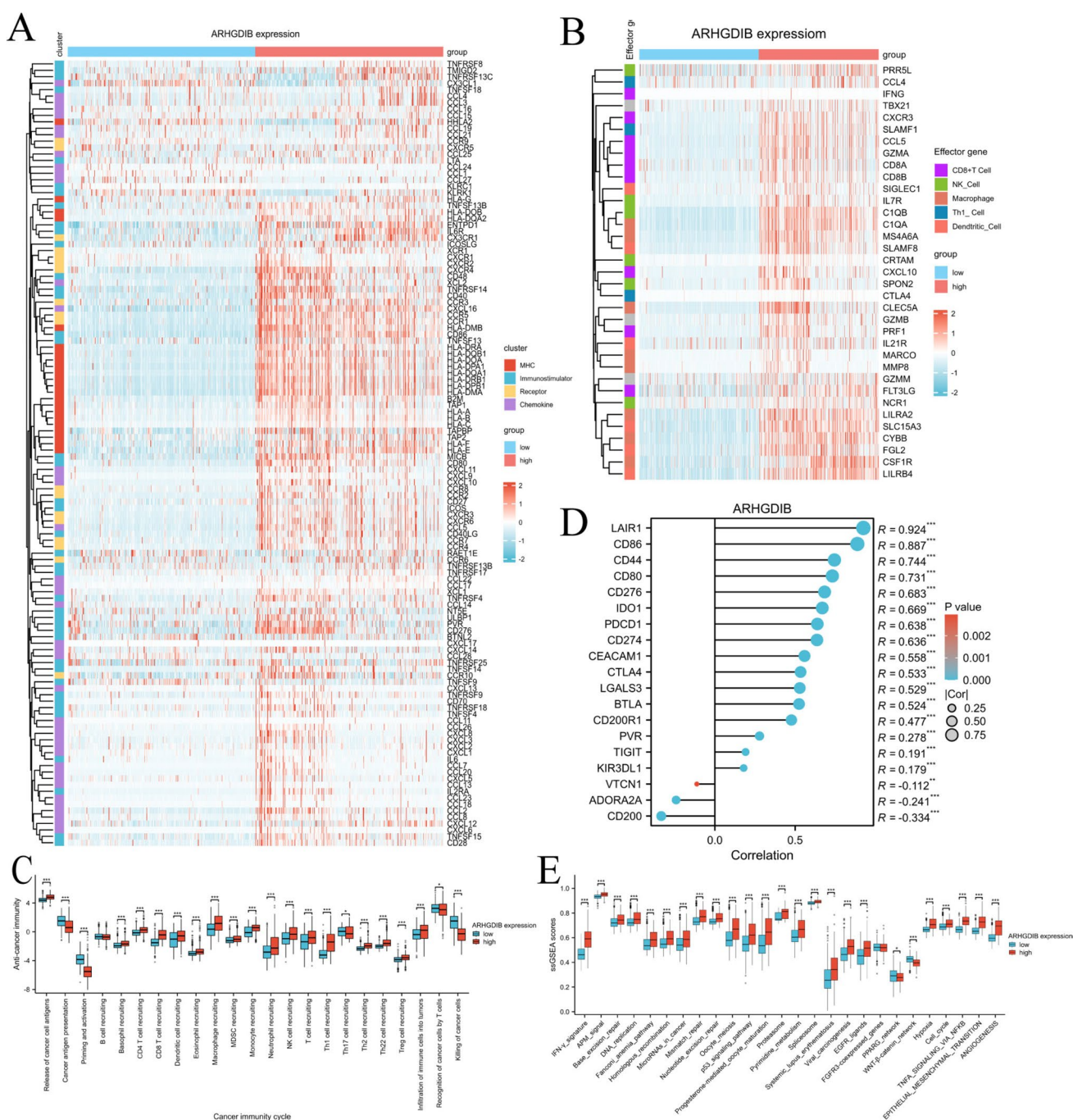
Fig. 4 ARHGDIB impairs the immune response in glioma. **A** Variations in the expression levels of 122 immunomodulatory molecules (including chemokines, receptors, MHC molecules, and immune stimulators) between glioma samples with high and low ARHGDIB expression. **B** Differences in immune cell markers between the high-ARHGDIB and low-ARHGDIB groups in TCGA cohort. **C** Differences in the various stages of the cancer immunity cycle between gliomas with high ARHGDIB expression and those with low ARH-GDIB expression in TCGA cohort. **D** The lollipop plot shows the correlation between the expression levels of 20 immune checkpoint molecules and the expression levels of ARHGDIB in TCGA cohort. **E** Differences in the enrichment scores of immunotherapy-related pathways between the high-ARHGDIB and low-ARHGDIB groups in the TCGA cohort. Differences between the two groups were assessed using Student's t test, with P values indicated above each boxplot using asterisks (**$P < 0.01$, ***$P < 0.001$)

(Fig. 6F). In addition, when glioma cells were cocultured with M0 macrophages overexpressing ARHGDIB, we found

that M0 macrophages overexpressing ARHGDIB promoted the proliferation and migration of T98G and U251 glioma
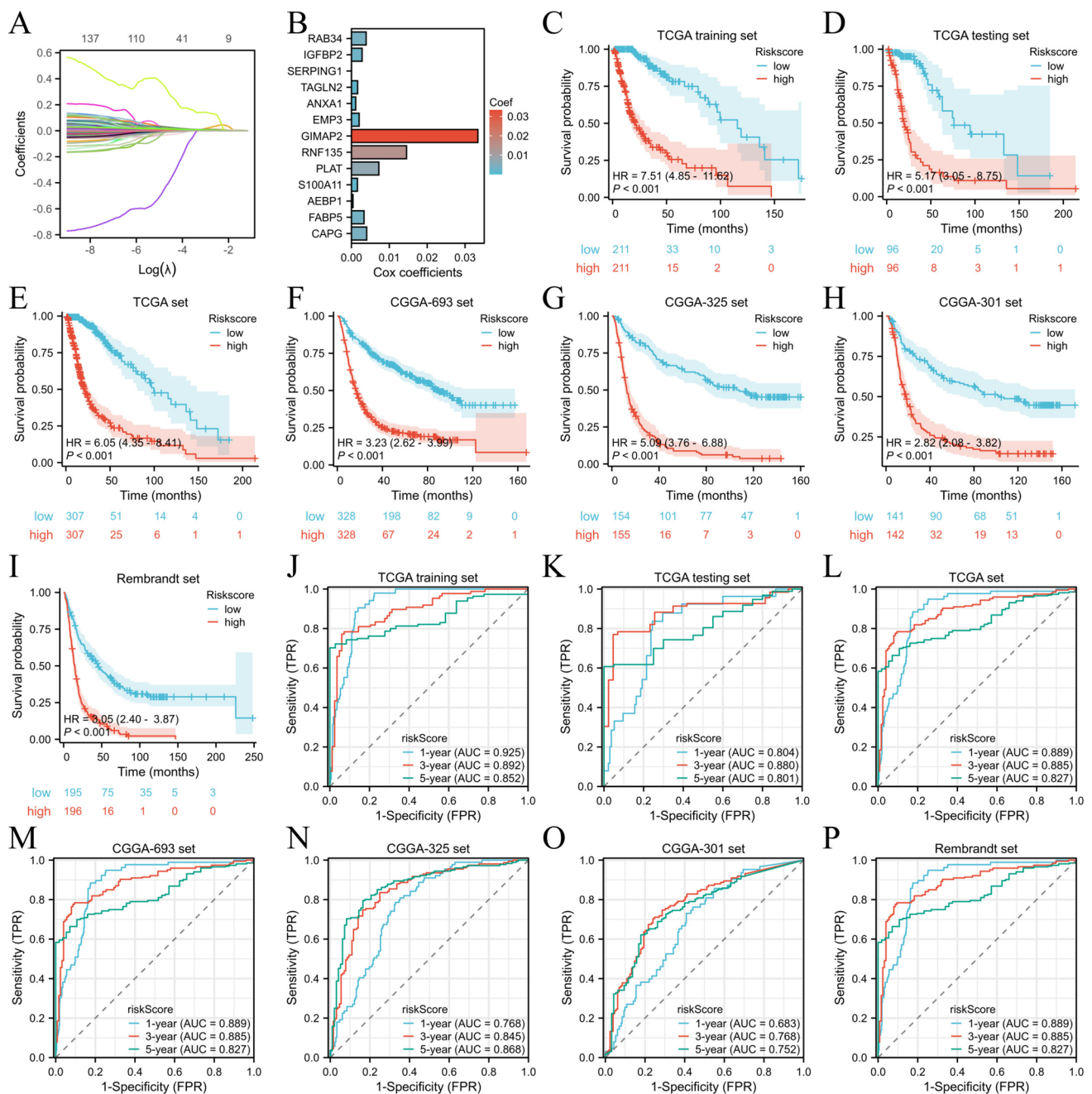
Fig. 5 Construction, validation, and assessment of the ARHGDIB-associated risk score. **A** The distribution of partial likelihood deviance for the LASSO coefficient. **B** A compilation of 13 ARHGDIB-associated signatures derived from Cox regression coefficients. **C–I** Kaplan–Meier curves demonstrate the correlation between risk scores and overall survival in various cohorts: TCGA training set (**C**), TCGA internal validation set (**D**), entire TCGA set (**E**), CGGA-693 cohort (**F**), CGGA-301 (**G**), CGGA-325 (**H**), and Rembrandt (**I**). *P* values were determined using the log-rank test, with *P* < 0.05 as the significance threshold. **J–P** Time-dependent ROC analysis for 1-year, 3-year, and 5-year survival demonstrated the predictive accuracy of the ARHGDIB-associated prognostic model across multiple cohorts: **J** TCGA training set, **K** TCGA internal validation set, **L** entire TCGA set, **M** CGGA-693 cohort, **N** CGGA-301, **O** CGGA-325, and **P** Rembrandt cohort
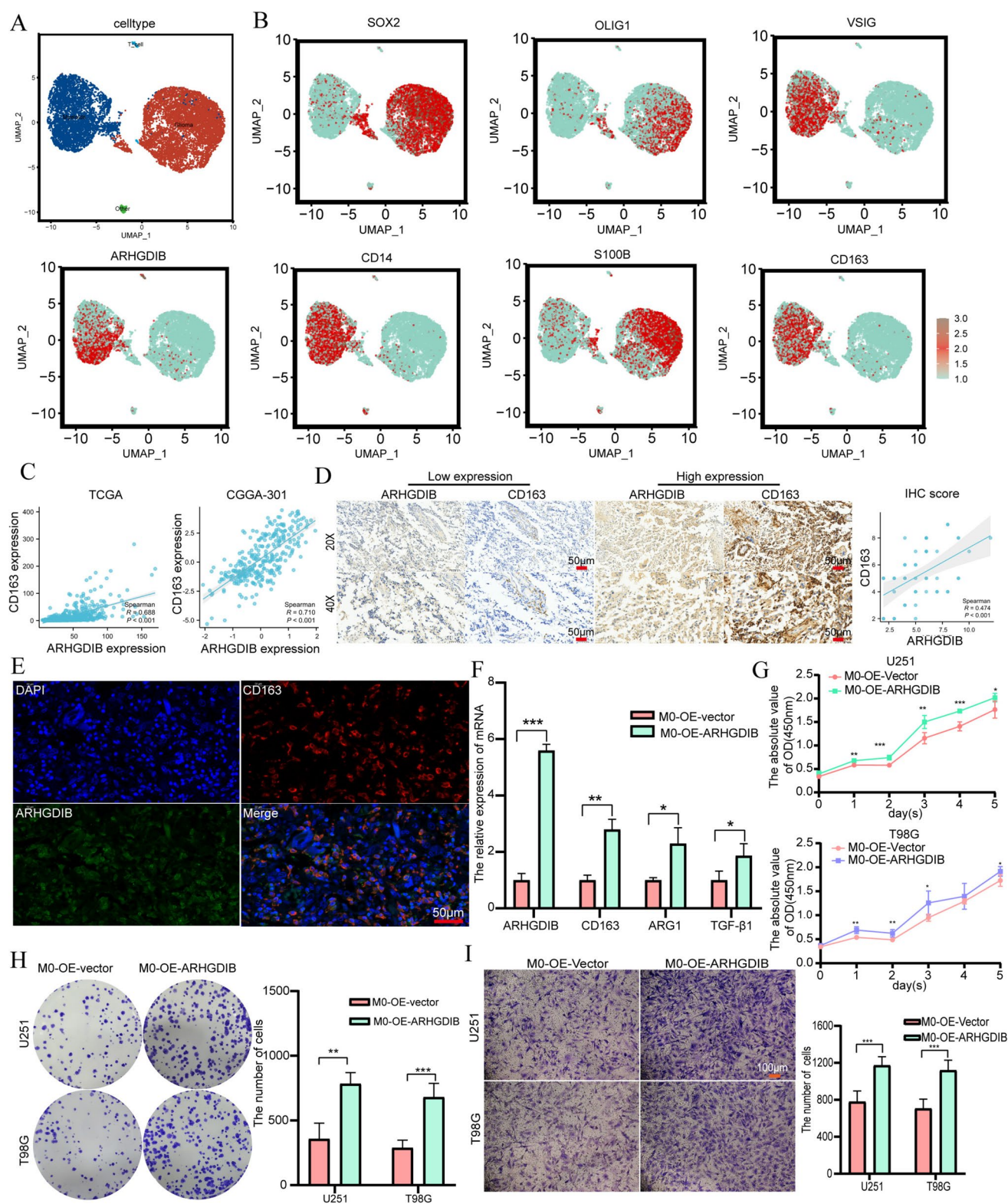
◄**Fig. 6** ARHGDIB induces M2 polarization of macrophages, thereby promoting the proliferation and migration of glioma cells. **A** single-cell sequencing analysis to identify four major cell types in glioma. **B** The distribution of ARHGDIB and markers of M2 macrophages and glioma cells in cell clusters. **C** Scatter plot showing the correlation of mRNA expression levels between ARHGDIB and CD163 in glioma samples from TCGA and CGGA-693 datasets. **D** The results of the immunohistochemical stain show the correlation of protein expression levels between ARHGDIB and CD163 in glioma tissues. **E** Immunofluorescence demonstrates the co-localization of ARHGDIB and CD163 in glioma tissues (scale bar: 50 μm). **F** qPCR analysis of M2 markers (CD163, ARG1, TGF-β) in M0 macrophages transfected with ARHGDIB or control vectors. **G–I** Co-culture systems were used to evaluate the effects on the proliferation and migration abilities of T98G and U251 cells after co-culture with M0 cells transfecting with ARHGDIB expression vectors or control vectors: **G** proliferation: T98G and U251 glioma cells were co-cultured with ARHGDIB-overexpressing M0 macrophages, proliferation was measured by CCK-8 assay at 1, 2, 3, 4, and 5 days (n = 5 replicates), **H** colony formation: cells were fixed with 4% PFA and stained with 0.1% crystal violet after 14 days, **I** cell migration was quantified using Transwell chambers; membranes were fixed with 4% PFA and stained with 0.1% crystal violet (scale bar: 100 μm). Data are presented as mean ± SD, and differences between the two groups were assessed using Student's t test, with P values indicated above each boxplot using asterisks (**$P < 0.01$, ***$P < 0.001$)

cells (Fig. 6G–I, $P < 0.001$). Taken together, the aberrant expression of ARHGDIB, which recruits the infiltration of M2 macrophages, promotes the malignant progression of glioma.

Discussion

Glioma is one of the most aggressive and heterogeneous brain tumors, characterized by poor prognosis and significant resistance to conventional therapies [37, 38]. Identifying novel biomarkers and therapeutic targets is crucial for improving patient outcomes. In this study, we revealed a significantly higher expression of ARHGDIB in glioma through comprehensive RNA sequencing and multi-cohort validation, and this finding was further validated in our internal cohort through qPCR and IHC (Fig. 1). In addition, the higher the malignancy of glioma, the higher the expression level of ARHGDIB. For example, compared with IDH-mutant and WHO grade 2 and 3 gliomas, ARHGDIB expression is higher in IDH wild-type and WHO grade 4 gliomas (Figure S1). These findings suggest that ARHGDIB may serve as a potential biomarker for the malignant features of gliomas. Previous studies have reported that ARHGDIB is significantly overexpressed in various types of cancers, such as gastric cancer, colorectal cancer, breast cancer, and melanoma [19, 20, 39]. These findings indicate that ARHGDIB may promote tumor progression, which is consistent with the conclusions of our study. Moreover, ARHGDIB is found to be a potential adverse prognostic biomarker for glioma patients, with its high expression being associated with a poor prognosis (Fig. 2). We also constructed a risk score model based on ARHGDIB-related prognostic genes, which is capable of accurately assessing the prognosis of glioma; patients with low-risk scores demonstrated significantly longer overall survival (Fig. 5). Taken together, ARHGDIB may serve as a potential adverse prognostic indicator in glioma patients. The underlying mechanisms of this association warrant further investigation. Certain molecular pathways or cellular processes may be dysregulated, leading to the increased expression of ARHGDIB and subsequent unfavorable outcomes. Regarding the utilization of ARHGDIB expression levels for optimizing treatment regimens, it could potentially serve as a guide for personalized medicine. For instance, patients with high ARHGDIB expression might benefit from more aggressive treatment approaches or novel therapeutic strategies. However, further studies are needed to determine the most effective treatment modalities based on ARHGDIB expression.

The glioma immune microenvironment is a complex immunosuppressive environment, characterized by a low abundance of immune cell infiltration, the presence of immunosuppressive cells, and high expression of immune checkpoint molecules [40]. These features significantly limit the efficacy of traditional therapeutic approaches, including chemotherapy, radiotherapy, and immunotherapy. In recent years, research has gradually unveiled the complexity and dynamic changes of the glioma immune microenvironment, providing a theoretical basis for the development of new therapeutic strategies [41, 42]. In this study, through GSEA (Gene Set Enrichment Analysis), we found that the highly expressed genes associated with ARHGDIB are mainly enriched in signaling pathways such as angiogenesis, inflammatory response, and TNF-α-NF-κB (Fig. 3B). Previous studies have reported that the blood vessels within tumors are characterized by high permeability and immaturity, leading to a hypoperfused and hypoxic environment within the tumor, which restricts the infiltration of immune cells, such as cytotoxic T cells, and promotes the accumulation of immunosuppressive cells, including regulatory T cells (Tregs), myeloid-derived suppressor cells (MDSCs), and M2-type tumor-associated macrophages (TAMs) [43, 44]. The TNF-α-NF-κB signaling pathway plays a crucial role in remodeling the glioma immunosuppressive microenvironment. Studies have reported that the TNF-α-activated NF-κB signaling pathway upregulates the expression of various pro-angiogenic factors (such as VEGF and IL-8), thereby promoting angiogenesis in gliomas [45]. This abnormal angiogenesis further reshapes the glioma microenvironment. Additionally, NF-κB promotes the polarization of TAMs toward the immunosuppressive phenotype (M2 type), thereby inhibiting anti-tumor immune responses [46]. Activation of the NF-κB

pathway can promote the infiltration of immunosuppressive cells by regulating the expression of cytokines (such as IL-8) and suppress the function of cytotoxic T cells to promote immune evasion of tumor cells by upregulating the expression of immune checkpoint molecules such as PD-L1 [45]. Incorporating our research findings, it is suggested that ARHGDIB is involved in the remodeling of the glioma immune microenvironment.

The results of the immune infiltration analysis showed that in glioma tissues with high expression of ARHGDIB, the immune cell and stromal cell scores were significantly higher than those in the group with low expression of ARHGDIB (Fig. 3C–H), indicating that ARHGDIB can regulate the infiltration of stromal cells and immune cells in gliomas microenvironment. Moreover, the high expression of ARHGDIB is closely associated with the infiltration of immunosuppressive cells. In glioma tissues with high expression of ARHGDIB, the infiltration levels of tumor-associated macrophages (TAMs), myeloid-derived suppressor cells (MDSCs), dendritic cells (DCs), and neutrophils are significantly higher than those in tissues with low expression of ARHGDIB (Fig. 3N–S). TAMs are one of the most important myeloid cells in the glioma microenvironment, characterized by their heterogeneity and plasticity. Among them, M2-type TAMs promote immune evasion by secreting immunosuppressive factors (such as TGF-β and IL-10) and downregulating the expression of MHC-I molecules, thereby inhibiting the activation of T cells [47–49]. Previous studies have found that neutrophils suppress the activity of T cells by secreting arginase and reactive oxygen species (ROS), thereby facilitating immune evasion. In addition, matrix metalloproteinases (such as MMP9) and cytokines (such as IL-8) secreted by neutrophils can promote tumor angiogenesis [50]. These mechanisms collectively act on the tumor microenvironment, influencing tumor progression and immune response. These research findings are consistent with our discoveries that ARHGDIB expression was positively correlated with the infiltration of immunosuppressive cells, such as M2 macrophages and neutrophils, while negatively correlated with antitumor immune cells like CD8+T cells and NK cells. These research findings indicate that high expression of ARHGDIB contributes to the formation of an immunosuppressive microenvironment in gliomas, thereby promoting tumor malignancy and leading to poor prognosis in patients.

The tumor immune response is a complex, multistep process that involves the release, and presentation of tumor antigens, activation of immune cells, their infiltration, and the killing of tumor cells [51]. However, gliomas are highly heterogeneous and characterized by an immunosuppressive microenvironment, which inhibits the immune response at multiple stages [52]. These research findings indirectly corroborate the accuracy of

our results that ARHGDIB-high gliomas exhibit impaired immune response at multiple stages, including antigen release, immune cell activation, recruitment, and killing of cancer cells (Fig. 4C). This indicates that patients with high expression of ARHGDIBG may achieve immune tolerance by inhibiting these aspects of the tumor immune response. Therefore, it is necessary to design personalized precision therapies for glioma patients with high expression of ARHGDIB to improve the efficacy of immunotherapy. Furthermore, elevated expression of ARHGDIB was also associated with increased levels of immunotherapy-related signatures and immune checkpoint molecules (Fig. 4D–E). Particularly, ARHGDIB in gliomas is highly positively correlated with most immune checkpoint molecules, including LAIR1, PDCD1, CD274, CD44, and CTLA-4 (Fig. 4D). Studies have found that upregulation of LAIR1 increases the expression of immunosuppressive chemokines/cytokines (such as CCL5, TGFβ2, and IL33), which promotes the polarization of macrophages and thereby forms an immunosuppressive microenvironment in gliomas [53]. LAIR1 is a novel immune checkpoint molecular; blocking the LAIR1 signaling pathway can enhance the antitumor immune response [54]. Although PD-1/PD-L1 inhibitors have achieved significant therapeutic efficacy in other types of tumors, their monotherapy efficacy in gliomas is limited. [55]. However, the immunosuppressive microenvironment of gliomas leads to the limited efficacy of immunotherapy with immune checkpoint inhibitors. Therefore, combination therapy strategies have become the focus of research [52]. The expression level of ARHGDIB is positively correlated with immune checkpoint molecules, indicating that the high expression of ARHGDIB in gliomas may be associated with the upregulation of immune checkpoint molecules (such as PD-L1), which may limit the efficacy of immune checkpoint inhibitor (ICB) therapy. In addition, ARHGDIB may induce resistance to immunotherapy in gliomas by promoting the formation of an immunosuppressive microenvironment. Therefore, ARHGDIB may serve as a potential target for immunotherapy, with the potential to enhance the efficacy of immunotherapy for glioma patients by developing small-molecule inhibitors or immune modulators targeting ARHGDIB.

Clinically, ARHGDIB IHC scoring could refine risk stratification, identifying patients who may benefit from intensified therapies or novel combinations. For example, ARHGDIB-high gliomas, characterized by PD-L1hi/M2hi TMEs, might exhibit primary resistance to PD-1 monotherapy but respond to combinations with CSF1-R inhibitors or macrophage-reprogramming agents. This aligns with emerging paradigms in melanoma and sarcoma, where TAM-targeted therapies synergize with checkpoint blockade. Furthermore, ARHGDIB itself represents a druggable node,

inhibiting its interaction with Rho GTPases or NF-κB could disrupt immunosuppressive signaling. While challenges like blood–brain barrier penetration and toxicity require optimization, our findings underscore ARHGDIB's dual role as a prognostic biomarker and immunotherapeutic target in glioma.

Our findings suggest that ARHGDIB drives M2 macrophage polarization via NF-κB activation and Rho GTPase dysregulation. In glioma-associated macrophages, ARHGDIB may potentiate TNFα-NF-κB signaling, enhancing the secretion of TGF-β and IL-10, which promote immunosuppression. Additionally, ARHGDIB's role as a RhoGDI could disrupt the balance of Rac1/RhoA activity, favoring STAT3/STAT6 pathways that drive M2 marker expression (e.g., CD163, ARG1). This aligns with studies showing Rac1-dependent NF-κB activation in M2 polarization. Future work should validate these pathways using ARHGDIB-knockdown models and pathway-specific inhibitors (e.g., NF-κB inhibitors). While our data implicate NF-κB and Rho GTPase pathways in ARHGDIB-mediated M2 polarization, direct evidence (e.g., phospho-NF-κB/STAT3 staining, Rho activity assays) is needed. Single-cell RNA-seq of ARHGDIB-high macrophages could further resolve pathway-specific signatures.

In recent years, the application of single-cell sequencing technology has provided new means for revealing tumor heterogeneity [30, 56]. In-depth studies on the role of ARHGDIB in different immune cell subsets using single-cell sequencing analysis will help elucidate its specific functions in glioma progression. In this study, based on the analysis of glioma single-cell sequencing data from GSE182905 [57], it was identified that ARHGDIB and CD163, a marker of M2 macrophage, have a common expression pattern. Immunofluorescence experiments demonstrated the co-localization of ARHGDIB and CD163. In vitro co-culture experiments showed that ARHGDIB induces M2 polarization of macrophages, which promotes the proliferation and migration of glioma cells (Fig. 6). Previous studies have indicated that M2 macrophages induce TMZ resistance in glioma and promote the proliferation and migration of tumor cells by secreting specific cytokines and chemokines, thereby exhibiting pro-tumorigenic properties in glioma [58, 59]. These findings suggest that ARHGDIB-mediated recruitment of M2 macrophages is a key mechanism underlying its pro-tumorigenic effects in glioma. Therefore, further exploring the specific molecular mechanisms by which ARHGDIB induces M2 polarization of macrophages to promote the proliferation and migration of glioma cells, and developing inhibitors targeting ARHGDIB to reverse M2 macrophage polarization in combination with immune checkpoint inhibitors, offer a new strategy for improving the efficacy of glioma immunotherapy.

Nevertheless, our study has several limitations. First, the lack of in vivo validation limits our understanding of ARHGDIB's systemic effects, particularly its interaction with the blood–brain barrier and non-myeloid cells. Second, while we propose NF-κB and Rho GTPase pathways as mechanistic drivers, direct evidence (e.g., phospho-protein assays) is needed to confirm causality. Third, reliance on bulk RNA-seq data and public cohorts may obscure subtype-specific or population-biased signals. For example, IDH-mutant gliomas, which exhibit distinct immune landscapes, were underrepresented in our analysis. Finally, the focus on M2 macrophages overlooks potential crosstalk with other immunosuppressive cells (e.g., Tregs), which may synergistically dampen anti-tumor immunity. Future work should integrate multi-omics approaches (e.g., single-cell proteomics) and preclinical models to resolve these gaps.

In conclusion, we utilized high-throughput sequencing technology, bioinformatics analysis, and in vitro experiments to discover that ARHGDIB is highly expressed in glioma and is closely related to tumor grading, serving as a biomarker for poor prognosis in glioma. ARHGDIB is involved in the remodeling of the glioma immune microenvironment. The abnormal expression of ARHGDIB recruits the infiltration of M2-type macrophages, forming an immunosuppressive microenvironment that promotes the malignant progression of the tumor. Additionally, ARHGDIB impairs the tumor immune response cycle, and its expression levels are associated with the PD-1/PD-L1 immune checkpoint molecules and the immunotherapy pathway. In summary, the role of ARHGDIB in the immunosuppressive microenvironment of glioma not only affects the biological behavior of the tumor and the response to immunotherapy but also provides new targets and strategies for future immunotherapy and personalized medicine.

Author contributions X.Y, X.J, C.R, and Q.Z were responsible for conceiving and designing the study as well as analyzing the results. J.X, H.L, and M.H. participated in the analysis procedures. X.Y wrote the manuscript, R.L. was responsible for creating the figures, and X.J and Q.Z contributed materials and funding. All authors participated in editing the manuscript and have reviewed and approved the final version for publication.

Data availability The data used in this study can be directly obtained online as described in the Materials and Methods section.

Declarations

Conflict of interest The authors declare that the research was conducted without any commercial or financial relationships that could be perceived as a potential conflict of interest.

Ethical approval All patients provided informed consent, and the ethics committee of XiangyaHospital, Central South University approved this study.

References

1. Louis DN, Perry A, Reifenberger G, von Deimling A, Figarella-Branger D, Cavenee WK et al (2016) The 2016 world health organization classification of tumors of the central nervous system: a summary. Acta Neuropathol 131(6):803–820

2. Okamoto Y, Di Patre PL, Burkhard C, Horstmann S, Jourde B, Fahey M et al (2004) Population-based study on incidence, survival rates, and genetic alterations of low-grade diffuse astrocytomas and oligodendrogliomas. Acta Neuropathol 108(1):49–56

3. Wang L, Gu M, Zhang X, Kong T, Liao J, Zhang D et al (2025) Recent advances in nanoenzymes based therapies for glioblastoma: overcoming barriers and enhancing targeted treatment. Adv Sci (Weinh) 24:e2413367

4. Stupp R, Mason WP, van den Bent MJ, Weller M, Fisher B, Taphoorn MJ et al (2005) Radiotherapy plus concomitant and adjuvant temozolomide for glioblastoma. N Engl J Med 352(10):987–996

5. Martínez-Ricarte F, Mayor R, Martínez-Sáez E, Rubio-Pérez C, Pineda E, Cordero E et al (2018) Molecular diagnosis of diffuse gliomas through sequencing of cell-free circulating tumor DNA from cerebrospinal fluid. Clin Cancer Res 24(12):2812–2819

6. Brennan CW, Verhaak RG, McKenna A, Campos B, Noushmehr H, Salama SR et al (2013) The somatic genomic landscape of glioblastoma. Cell 155(2):462–477. https://doi.org/10.1016/j.cell.2013.09.034.Erratum.In:Cell.2014Apr24;157(3):753

7. Bao Z, Wang Y, Wang Q, Fang S, Shan X, Wang J et al (2021) Intratumor heterogeneity, microenvironment, and mechanisms of drug resistance in glioma recurrence and evolution. Front Med 15(4):551–561

8. Jayaram MA, Phillips JJ (2024) Role of the microenvironment in glioma pathogenesis. Annu Rev Pathol 24(19):181–201

9. Kzhyshkowska J, Shen J, Larionova I (2024) Targeting of TAMs: can we be more clever than cancer cells? Cell Mol Immunol 21(12):1376–1409

10. Sielska M, Przanowski P, Wylot B, Gabrusiewicz K, Maleszewska M, Kijewska M et al (2013) Distinct roles of CSF family cytokines in macrophage infiltration and activation in glioma progression and injury response. J Pathol 230(3):310–321

11. Pyonteck SM, Akkari L, Schuhmacher AJ, Bowman RL, Sevenich L, Quail DF et al (2013) CSF-1R inhibition alters macrophage polarization and blocks glioma progression. Nat Med 19(10):1264–1272

12. Fukata M, Kaibuchi K (2001) Rho-family GTPases in cadherin-mediated cell-cell adhesion. Nat Rev Mol Cell Biol 2(12):887–897

13. Guillemot JC, Kruskal BA, Adra CN, Zhu S, Ko JL, Burch P et al (1996) Targeted disruption of guanosine diphosphate-dissociation inhibitor for Rho-related proteins, GDID4: normal hematopoietic differentiation but subtle defect in superoxide production by macrophages derived from in vitro embryonal stem cell differentiation. Blood 88(7):2722–2731

14. Tripathi M, Colige A, Deroanne CF (2023) The dual function of RhoGDI2 in immunity and cancer. Int J Mol Sci 24(4):4015

15. Niu H, Li H, Xu C, He P (2010) Expression profile of RhoGDI2 in lung cancers and role of RhoGDI2 in lung cancer metastasis. Oncol Rep 24(2):465–471

16. Ma L, Xu G, Sotnikova A, Szczepanowski M, Giefing M, Krause K et al (2007) Loss of expression of LyGDI (ARHGDIB), a rho GDP-dissociation inhibitor. Hodgkin lymphoma Br J Haematol 139(2):217–223

17. Liu L, Cui J, Zhao Y, Liu X, Chen L, Xia Y et al (2021) KDM6A-ARHGDIB axis blocks metastasis of bladder cancer by inhibiting Rac1. Mol Cancer 20(1):77

18. Cho HJ, Baek KE, Park SM, Kim IK, Choi YL, Cho HJ et al (2009) RhoGDI2 expression is associated with tumor growth and malignant progression of gastric cancer. Clin Cancer Res 15(8):2612–2619

19. Zhang Y, Zhang B (2006) D4-GDI, a Rho GTPase regulator, promotes breast cancer cell invasiveness. Cancer Res 66(11):5592–5598

20. Li X, Wang J, Zhang X, Zeng Y, Liang L, Ding Y (2012) Overexpression of RhoGDI2 correlates with tumor progression and poor prognosis in colorectal carcinoma. Ann Surg Oncol 19(1):145–153

21. Fang Y, Yi J, Lizhi L, Qiucheng C (2014) Rho GDP dissociation inhibitor beta promotes cell proliferation and invasion by modulating the AKT pathway in hepatocellular carcinoma. DNA Cell Biol 33(11):781–786

22. Stevens EV, Banet N, Onesto C, Plachco A, Alan JK, Nikolaishvili-Feinberg N et al (2011) RhoGDI2 antagonizes ovarian carcinoma growth, invasion and metastasis. Small GTPases 2(4):202–210

23. Wang X, Bi X, Huang X, Wang B, Guo Q, Wu Z (2020) Systematic investigation of biomarker-like role of ARHGDIB in breast cancer. Cancer Biomark 28(1):101–110

24. Cho HJ, Baek KE, Nam IK, Park SM, Kim IK, Park SH et al (2011) PLCγ is required for RhoGDI2-mediated cisplatin resistance in gastric cancer. Biochem Biophys Res Commun 414(3):575–580

25. Cho HJ, Baek KE, Park SM, Kim IK, Nam IK, Choi YL et al (2011) RhoGDI2 confers gastric cancer cells resistance against cisplatin-induced apoptosis by upregulation of Bcl-2 expression. Cancer Lett 311(1):48–56

26. Sanchez-Carbayo M, Smith SC, Theodorescu D (2012) RhoGDI2 suppresses lung metastasis in mice by reducing tumor versican expression and macrophage infiltration. J Clin Invest 122(4):1503–1518

27. Zhou Q, Wei M, Shen W, Huang S, Fan J, Huang H (2022) SYK is associated with malignant phenotype and immune checkpoints in diffuse glioma. Front Genet 15(13):899883

28. Yan X, Zhou Q, Zhu H, Liu W, Xu H, Yin W et al (2021) The clinical features, prognostic significance, and immune heterogeneity of CD37 in diffuse gliomas. iScience 24(11):103249

29. Xu H, Yan X, Zhu H, Kang Y, Luo W, Zhao J et al (2022) TBL1X and Flot2 form a positive feedback loop to promote metastasis in nasopharyngeal carcinoma. Int J Biol Sci 18(3):1134–1149

30. Zhou Q, Yan X, Guo Y, Jiang X, Cao T, Ke Y (2024) Machine learning algorithms for predicting glioma patient prognosis based on CD163+FPR3+ macrophage signature. NPJ Precis Oncol 8(1):201

31. Yoshihara K, Shahmoradgoli M, Martínez E, Vegesna R, Kim H, Torres-Garcia W et al (2013) Inferring tumour purity and stromal and immune cell admixture from expression data. Nat Commun 4:2612

32. Li S, Guo Y, Hu H, Gao N, Yan X, Zhou Q et al (2023) TANK shapes an immunosuppressive microenvironment and predicts prognosis and therapeutic response in glioma. Front Immunol 5(14):1138203

33. Barbie DA, Tamayo P, Boehm JS, Kim SY, Moody SE, Dunn IF et al (2009) Systematic RNA interference reveals that oncogenic KRAS-driven cancers require TBK1. Nature 462(7269):108–112

34. Newman AM, Liu CL, Green MR, Gentles AJ, Feng W, Xu Y et al (2015) Robust enumeration of cell subsets from tissue expression profiles. Nat Methods 12(5):453–457

35. Auslander N, Zhang G, Lee JS, Frederick DT, Miao B, Moll T et al (2018) Robust prediction of response to immune checkpoint blockade therapy in metastatic melanoma. Nat Med 24(10):1545–1549

36. Hu J, Yu A, Othmane B, Qiu D, Li H, Li C et al (2021) Siglec15 shapes a non-inflamed tumor microenvironment and predicts the molecular subtype in bladder cancer. Theranostics 11(7):3089–3108

37. Janjua TI, Rewatkar P, Ahmed-Cox A, Saeed I, Mansfeld FM, Kulshreshtha R et al (2021) Frontiers in the treatment of glioblastoma: past, present and emerging. Adv Drug Deliv Rev 171:108–138. https://doi.org/10.1016/j.addr.2021.01.012. (**Epub 2021 Jan 21**)

38. Hawly J, Murcar MG, Schcolnik-Cabrera A, Issa ME (2024) Glioblastoma stem cell metabolism and immunity. Cancer Metastasis Rev 43(3):1015–1035

39. Kim HJ, Ryu KJ, Kim M, Kim T, Kim SH, Han H et al (2022) RhoGDI2-mediated rac1 recruitment to filamin a enhances rac1 activity and promotes invasive abilities of gastric cancer cells. Cancers (Basel) 14(1):255. https://doi.org/10.3390/cancers14010255

40. Lu J, Huo W, Ma Y, Wang X, Yu J (2024) Suppressive immune microenvironment and CART therapy for glioblastoma: future prospects and challenges. Cancer Lett 28(600):217185

41. Foray C, Valtorta S, Barca C, Winkeler A, Roll W, Müther M et al (2021) Imaging temozolomide-induced changes in the myeloid glioma microenvironment. Theranostics 11(5):2020–2033

42. Dong F, Qin X, Wang B, Li Q, Hu J, Cheng X et al (2021) ALKBH5 facilitates hypoxia-induced paraspeckle assembly and IL8 secretion to generate an immunosuppressive tumor microenvironment. Cancer Res 81(23):5876–5888

43. Hadjigeorgiou AG, Stylianopoulos T (2024) Hybrid model of tumor growth, angiogenesis and immune response yields strategies to improve antiangiogenic therapy. NPJ Biol Phys Mech 1(1):4

44. Liu ZL, Chen HH, Zheng LL, Sun LP, Shi L (2023) Angiogenic signaling pathways and anti-angiogenic therapy for cancer. Signal Transduct Target Ther 8(1):198

45. Khan A, Zhang Y, Ma N, Shi J, Hou Y (2024) NF-κB role on tumor proliferation, migration, invasion and immune escape. Cancer Gene Ther 31(11):1599–1610. https://doi.org/10.1038/s41417-024-00811-6. (**Epub 2024 Jul 20**)

46. He R, He Y, Du R, Liu C, Chen Z, Zeng A, Song L (2023) Revisiting of TAMs in tumor immune microenvironment: Insight from NF-κB signaling pathway. Biomed Pharmacother 165:115090

47. Li J, Wang K, Yang C, Zhu K, Jiang C, Wang M et al (2023) Tumor-associated macrophage-derived exosomal LINC01232 induces the immune escape in glioma by decreasing surface MHC-I expression. Adv Sci (Weinh) 10(17):2207067

48. Li D, Zhang Q, Li L, Chen K, Yang J, Dixit D et al (2022) β2-microglobulin maintains glioblastoma stem cells and induces M2-like polarization of tumor-associated macrophages. Cancer Res 82(18):3321–3334

49. Prosniak M, Harshyne LA, Andrews DW, Kenyon LC, Bedelbaeva K, Apanasovich TV et al (2013) Glioma grade is associated with the accumulation and activity of cells bearing M2 monocyte markers. Clin Cancer Res 19(14):3776–3786

50. Wen J, Liu D, Zhu H, Shu K (2024) Microenvironmental regulation of tumor-associated neutrophils in malignant glioma: from mechanism to therapy. J Neuroinflammation 21(1):226

51. Chen DS, Mellman I (2013) Oncology meets immunology: the cancer-immunity cycle. Immunity 39(1):1–10

52. Lin H, Liu C, Hu A, Zhang D, Yang H, Mao Y (2024) Understanding the immunosuppressive microenvironment of glioma: mechanistic insights and clinical perspectives. J Hematol Oncol 17(1):31

53. Wei X, Pan S, Wang Z, Chen J, Lu L, Cao Q et al (2023) LAIR1 drives glioma progression by nuclear focal adhesion kinase dependent expressions of cyclin D1 and immunosuppressive chemokines/cytokines. Cell Death Dis 14(10):684

54. Rodriguez BL, Huang J, Gibson L, Fradette JJ, Chen HH, Koyano K et al (2024) Antitumor activity of a novel LAIR1 antagonist in combination with anti-PD1 to treat collagen-rich solid tumors. Mol Cancer Ther 23(8):1144–1158

55. Jiacheng D, Jiayue C, Ying G, Shaohua W, Wenhui L, Xinyu H (2024) Research progress and challenges of the PD-1/PD-L1 axis in gliomas. Cell Biosci 14(1):123

56. Ochocka N, Segit P, Walentynowicz KA, Wojnicki K, Cyranowski S, Swatler J et al (2021) Single-cell RNA sequencing reveals functional heterogeneity of glioma-associated brain macrophages. Nat Commun 12(1):1151

57. Abdelfattah N, Kumar P, Wang C, Leu JS, Flynn WF, Gao R et al (2022) Single-cell analysis of human glioma and immune cells identifies S100A4 as an immunotherapy target. Nat Commun 13(1):767

58. Kricha A, Bouchmaa N, Ben Mkaddem S, Abbaoui A, Ben Mrid R, El Fatimy R (2024) Glioblastoma-associated macrophages: a key target in overcoming glioblastoma therapeutic resistance. Cytokine Growth Factor Rev 80:97–108

59. Cao W, Zeng Z, Sun J, Chen Y, Kuang F, Luo S et al (2024) Exosome-derived circ-001422 promotes tumor-associated macrophage M2 polarization to accelerate the progression of glioma. Commun Biol 7(1):1504